Journal of Water and Climate Change | 01.1 | 2010

Modeling river discharge rates in California watersheds

Christopher Potter, John Shupe, Peggy Gross, Vanessa Genovese and Steven Klooster

ABSTRACT

River discharge rates across all California's watershed have been modeled using the NASA version of the Carnegie-Ames-Stanford Approach (CASA) ecosystem model coupled with a surface hydrologic routing scheme previously called the Hydrological Routing Algorithm (HYDRA). To assess CASA-HYDRA's capability to estimate actual water flows in extreme and non-extreme precipitation years, we have organized hundreds of California river gauge records for comparison to monthly model predictions. Previously, CASA-HYDRA snowmelt algorithms were modified with equations from the USDA Snowmelt Runoff Model, which has been designed to predict daily stream flow in mountain basins where snowmelt is a major runoff factor. Based on model predictions of monthly flow rates across 336 stream gauges statewide, the multi-year model-to-measurement correlation between monthly river flow rates was $R^2 = 0.72$. The model output was 15% higher across all these stream gauges than the measured monthly flow records for 1982–1990. It is plausible that the model would predict higher flow rates statewide than was measured at many gauge locations, due mainly to extensive water diversions for power generation and crop irrigation in the valley growing regions of the state. Predictions for gauges located on the state's North Coast and Sierra regions showed errors distributed fairly evenly throughout the seasons, whereas results for Central Coast and Southern regions showed higher errors mainly during the summer and fall. Future model applications for land cover and climate change in California are outlined.

Key words | forests, irrigation, rangelands, water allocation, water supply, watershed management

Christopher Potter (corresponding author)
NASA Ames Research Center,
Moffett Field, CA,
USA
Tel.: 650-604-6164
Fax: 650-604-468
E-mail: *chris.potter@nasa.gov*

John Shupe
Peggy Gross
Vanessa Genovese
Steven Klooster
California State University Monterey Bay,
Seaside, CA,
USA

ABBREVIATIONS AND NOTATIONS

HYDRA	Hydrological Routing Algorithm (large-scale hydrologic model)
THMB	Terrestrial Hydrology Model with Biogeochemistry (previously termed HYDRA)
CASA	Carnegie-Ames-Stanford Approach
SST	Sea Surface Temperature
ENSO	El Niño Southern Oscillation
PDO	Pacific Multi-Decadal Oscillation
GCM	general circulation model
DEM	Digital Elevation Model
ET	Evapotranspiration
SRM	Snowmelt Runoff Model
S_m	Potential snow melt (cm)
a	degree-day factor (cm/°C·day)
T	degree-days (°C·day)
R^2	Pearson product-moment correlation coefficient
VIC	Variable Infiltration Capacity
CALVIN	California Value Integrated Network
HEC-PRM	Hydrological Engineering Center Prescriptive Reservoir Model
RMSE	Root Mean Square Error

doi: 10.2166/wcc.2010.012

INTRODUCTION

The pathways and processes that affect runoff generation from a watershed result from a complex interaction of climate, topography, soils, land cover, and land use. Since land cover influences soil moisture storage, water infiltration rates, and transpiration rates, differences in cover classification may strongly impact the simulation of runoff when using a watershed computer model. For instance, the amount of forest versus non-forest cover modifies and moderates many hydrologic factors within a watershed. The absence of forest and shrub cover in a watershed implies a minimum in surface evapotranspiration and, consequently, a maximum in runoff, with the opposite occurring in the case of continuous, deeply rooted forest cover in a watershed.

In a global study of the world's 30 largest river basins, Potter *et al.* (2004) characterized surface hydrologic flows in relation to net precipitation inputs and anthropogenic water use patterns related to land cover. Based on findings from 20 years of climate and river flow records, cropland development and irrigation diversions could best explain the inter-annual patterns in monthly discharge rates for at least one-third of the 30 major river drainages in the global discharge dataset.

On smaller scales, Miller *et al.* (2002) described simulated stream flow impacts in response to historical land use shifts for watersheds in Arizona and New York, USA. Stream flows were predicted to increase due to increased urban and agricultural land use, while a shift from agricultural to forest land use was predicted to result in lower stream flow. Cao *et al.* (2008) found that under current land use conditions in New Zealand, both annual water yield and low flow are higher than in simulations of cover conditions that preceded human land use change or in a maximum commercial reforestation scenario. In a generalized modeling study, Miller *et al.* (2007*a*,*b*) reported that as watershed size and storm size increase, the impacts of land cover classification errors on predicted runoff from hydrologic models decrease.

Understanding the interacting effects of climate and land use on river flow rates is a necessary first step towards addressing a broader list of environmental concerns for California's river systems. Of chief concern are agricultural, forestry, and urban contributions to surface water quantity and quality, accelerated soil erosion and sedimentation of floodplains, increased risk of flood, and maintenance of water management operations at the state's many reservoirs.

This study is the first presentation of the coupling of a large-scale hydrologic model previously called HYDRA (Coe 2000; now called THMB: Terrestrial Hydrology Model with Biogeochemistry) to the Carnegie-Ames-Stanford Approach (CASA) terrestrial ecosystem model for application in California. Several advancements of the coupled CASA-HYDRA approach over previously published surface hydrology models have been described, including additional of satellite remote sensing of land surface conditions and refinements of soil water storage and snow melt dynamics. No other published modeling studies have used this unique combination of satellite remote sensing and surface runoff refinements to address statewide issues in water management.

Protection of water resources and the catchments from which it is derived remains critical to the environmental integrity of downstream areas. Large-scale hydrologic processes that could be impacted in California by climate shifts and land cover changes include: later onset of and reduced snowpacks, earlier snowmelt, more frequent flood events, higher evapotranspiration rates, more frequent and longer droughts, more frequent and more intense wildfires, reduced summer and fall stream flows, and the loss of riparian vegetation leading to further increase in stream temperature and soil loss. Simulation modeling is one way to begin to address the potential impacts of multiple environmental changes.

The main objectives of this study were to:

- Develop a statewide modeling approach for monthly surface water flows that can account for variations in climate, land cover, land use, and soil properties;
- Evaluate the modeled flow rates at all available station locations throughout the state with long-term gauge flow records;
- Evaluate the accuracy of the modeled flow rates (versus historical records) as a function of land cover mapping from satellites and the presence or absence of water management features (diversions and dams) in selected river basins.

Two hypotheses were tested in this study, which extend from the findings of previous papers cited above:

- Modeled flow rates are consistently more accurate (compared to historical river flow records) in watersheds where satellite mapping specifies a more homogeneous land cover composition (mainly forest or shrubland) than in watersheds with highly mixed agricultural and urbanized land cover types.
- Modeled flow rates are significantly less accurate (compared to historical flow records) in watersheds where river diversions for generation of hydroelectric power are prevalent, compared to rivers with no diversions for generation of hydroelectric power.

BACKGROUND ON CALIFORNIA'S SURFACE HYDROLOGY

California has a diverse landscape, made up of the widest range of climate, landforms, and rivers in the USA, as well as a long history of both extensive and intensive settlement and land use. From north to south, the state's surface hydrology is regulated by regional gradients of climate and human interventions. On average, more than 170 cm of precipitation falls annually in the mountains of northwestern California, while fewer than 10 cm falls in parts of the desert in the southeast portion of the State.

The North Coast hydrologic region is the wettest region of the state. Most of the precipitation falls as rain during winter storms, and persistent fog provides additional moisture throughout the summer. The basin's steep terrain results in a strong orographic effect along the coast. The steep terrain and unstable soils in the North Coast hydrologic region also result in the highest sediment yields in the state (Mount 1995).

California's Central Valley supports a diverse agricultural economy, much of which depends on the availability of irrigation water. In the mid-1990s, approximately 75% of statewide water consumption occurred in California's agricultural sector. Water is collected in reservoirs at several locations within the mountains surrounding the Central Valley and is released according to allocations for agricultural, urban, and environmental needs. The reservoirs also are managed for flood control and allow the storage of water during dry years.

Central California has a Mediterranean climate and, as a consequence, the majority of the precipitation falls in the winter and early spring (Lundquist *et al.* 2005). Correspondingly, runoff occurs primarily between December and March in the Sierra foothills and Central Valley. In the upper reaches of the Sierra region, which is dominated by snowfall, runoff from snowmelt typically occurs between April and July (SFCCPD 2007). Over half of California's water supply comes from the Sierra Nevada snowpack, so this contribution is critical to the state's water budget (Lundquist *et al.* 2005).

In southern California, precipitation is scarce and highly variable in time and space. The intensity and frequency of flooding in this part of the state has been related to upstream urban development (Callaway & Davis 1993). Where land cover has been converted from natural vegetation to built-up structures, the area of impervious ground cover and the velocity at which water runs off the land usually increase. Infiltration of precipitation into the soil decreases, causing more runoff and flooding during storms and reduced long-term recharge of soil moisture and aquifers.

Pacific Ocean sea surface temperatures (SSTs) affect low-frequency climate oscillations in California, namely the El Niño Southern Oscillation (ENSO) and the Pacific multi-Decadal Oscillation (PDO). ENSO has a 3–5 year cycle and is termed El Niño for its positive phase, and La Niña for its negative phase. The PDO responds to SST patterns in the northern, equatorial, and southern Pacific Ocean and has an approximately 30 year cycle. Major floods on California's rivers can be triggered by winter storm systems moving on-shore from the Pacific, and bringing moist subtropical air from a southwesterly direction into the State. A case in point is the 1986 flood on the American River, during which warmer-than-normal air temperatures and intense precipitation increased storm runoff by about 10% and caused more than a billion dollars in property damage.

Trend analyses on data from the 20 largest streams entering the Pacific Ocean along the central and southern California coast confirm that ENSO-induced climate changes recur on a multi-decadal time scale in general agreement with the Pacific/North American climate pattern (Inman & Jenkins 1999). As noted by Roos (1991), and later elaborated by Dettinger & Cayan (1995), the fraction of the annual runoff from the central Sierra that occurs in late spring has been decreasing for approximately the past 50 years. Relatively more of the annual runoff has been occurring in the winter. Winter and spring temperatures have become warmer in the central Sierra. Several modeling studies of surface hydrologic responses to climate change, including those from Knowles & Cayan (2002), Maurer & Duffy (2005) and Vicuna *et al.* (2007), have projected runoff trends across the State for decades into the future.

MODEL DEVELOPMENT OVERVIEW

The NASA-CASA is a model developed by Potter *et al.* (1993, 2007), which combines multi-year satellite and climate data from historical records or from general circulation models (GCMs) to estimate the biosphere–atmosphere exchange of energy, water, and trace gases from plants and soils. Soil water balance in CASA is controlled by land cover type and soil rooting zone depth settings that are both derived from NASA satellite data sets. Soil water moves through 3–4 surface layers that freeze and thaw in cold regions according to empirical temperature algorithms. Drainage outputs below the root zone are predicted. CASA's drainage and evapotranspiration outputs are used as inputs to the HYDRA surface routing model.

Overview of HYDRA model and 1-km downscaling

The program previously called the Hydrological Routing Algorithm (HYDRA) is a fully distributed computer model that can predict the flow of surface water in streams and rivers (Coe 2000). HYDRA uses a linear reservoir model to transport local surface runoff and subsurface drainage through a river network to inland basins, or directly to the ocean. The model simulates water transport in terms of river routing directions derived from local topography, residence times within a grid cell, and effective flow velocities.

The coupled CASA-HYDRA model simulates a set of physical hydrologic processes including interception, infiltration, interflow, base flow, overland routing, and channel routing, according to the parameterizations from Coe (2000). The CASA-HYDRA model uses river transport directions based on digital elevation model (DEM) representations of the land surface. River discharge is calculated at each grid cell as the accumulated flow of water across the drainage basin surface using 30-m DEM directional information. HYDRA can use inputs of monthly precipitation from interpolated weather station data sets, surface evapotranspiration (ET), snowmelt, and soil water retention from the CASA model. MODIS and Landsat satellite remote sensing products are used for the first time by CASA-HYDRA to define detailed land cover variations region-wide in the CASA-HYDRA model.

Modeled river routing and climate inputs

River and stream water routing pathways were mapped across the state starting from the 30-m resolution DEM provided by the US Geological Survey (USGS 2008). These pathways were aggregated to a 1-km resolution HYDRA grid for surface flow directions. Other spatial data sets used in the CASA-HYDRA model development were the NASA MODIS 1-km land cover map to set vegetation rooting depths, together with USDA STATSGO for soil water storage capacity based on CASA soil texture classification (Potter *et al.* 2007). In locations where the USDA data sets on "depth to bedrock" was specified as greater than 1.25 m, forest land cover from MODIS data were assigned a rooting depth of 2 m. Otherwise USDA "depth to bedrock" values were specified as maximum plant rooting depth.

Because many forest soils in California are relatively shallow and underlain by thick layers of weathered bedrock (Witty *et al.* 2003), the NASA-CASA model settings for soil water holding capacity were modified for coupled CASA-HYDRA simulations at high elevations. According to USDA depth to bedrock data, the forest rooting zone was set to 7 cm across the Sierra Nevada mountain range and maximum moisture holding capacity of surface soils was set at 0.27 cm per cm rooting depth (Potter *et al.* 2007). Precipitation and snowmelt water in the model could be utilized for evapotranspiration by forest cover in the Sierra region for a maximum of one month after entry into the simulated rooting zone, which would reflect the low moisture retention capacity of weathered bedrock layers where forest roots may nevertheless penetrate to 1 m depth (Witty *et al.* 2003).

Monthly climate data sets (surface temperature and precipitation) from DAYMET (Thornton *et al.* 1997) were used as CASA-HYDRA model inputs from 1982–1990. DAYMET algorithms are based on the spatial convolution of a truncated Gaussian weighting filter with the set of available weather station locations in a given region. Daily climate input data were not used to drive the CASA-HYDRA model because such accurately downscaled precipitation data (to at least 1-km spatial resolution) do not exist. Hence, the best option was to develop sub-monthly corrections to surface temperature and snowmelt simulations to compensate for the lack of daily historical precipitation climatologies at the statewide level.

Specifically, CASA-HYDRA snowmelt algorithms were modified with equations from the USDA Snowmelt Runoff Model (SRM), which has been designed to predict daily stream flow in mountain basins where snowmelt is a major runoff factor. The SRM was originally developed by Martinec (1975) for small European basins. Since then, the SRM has been applied in at least 80 basins situated in 25 different countries and in basins as large as 122,000 km^2. The SRM is a degree-day model that requires daily input for temperature, precipitation, and snow cover extent. Additionally, the model has eight parameters which can either be derived from measurements or estimated by hydrological knowledge, taking into account the local basin characteristics, physical laws, and theoretical or empirical relationships. The SRM degree-day algorithm has been incorporated into the CASA-HYDRA model as described in the following section.

NEW CASA-HYDRA FEATURES FOR SNOWMELT

Degree-day method

To improve CASA's snow melt algorithm, the following degree-day calculation was integrated into the model:

$$S_m = a \times T$$

where S_m is potential snow melt (cm), a is the degree-day factor (cm/°C·day) and T is the degree-days (°C·day). Essentially, the degree-day factor converts the number of degree-days into a potential snow melt depth. For the degree-day factor, values calculated by Rice *et al.* (2007) were adopted, based on their studies in the Tuolumne and Merced River watersheds.

CASA uses inputs of monthly temperature data, which makes it problematic to calculate degree-days because using average monthly temperatures has the propensity to underestimate the true degree-day total. This is due to the fact that a temperature below the melt threshold will not subtract from the cumulative total of degree-days, but it can lower the average temperature. We refer to this potential underestimation as the degree-day difference.

To develop a method for estimating the degree-day difference, we analyzed daily DAYMET temperature data for the months of November through February during the years 1980–2003. Data were collected at four points from the Merced River watershed in Yosemite National Park and five points from the American River watershed, which is a major tributary of the Sacramento River. The points in each watershed were chosen so that they represented the elevation range of the study area of each basin, which is about 1,200–4,000 m for the Merced River and about 800–3,000 m for the American River. Additionally, the basins were chosen so that they captured the variability of the Sierra Nevada. The American River is in the northern Sierra where elevations are lower but precipitation is more plentiful. The Merced River watershed is in the southern Sierra, which experiences less precipitation, but it includes the highest elevations seen in the continental United States.

Our analysis revealed that two independent variables explained most of the variance in the degree-day difference. These covariates are the average monthly temperature and the monthly temperature range. The scatter plot in Figure 1 shows the correlation between average monthly temperature and the degree-day difference. There is an obvious point of inflection at 3°C, which is the threshold that we used to calculate degree-days, since it is the typical temperature at which snow melts early in the season (Martinec *et al.* 1998). Using non-linear regression (Freund *et al.* 2003), average monthly temperature by itself explains approximately 0.62 of the variance to the left of the inflection point and 0.74 to the right of it.

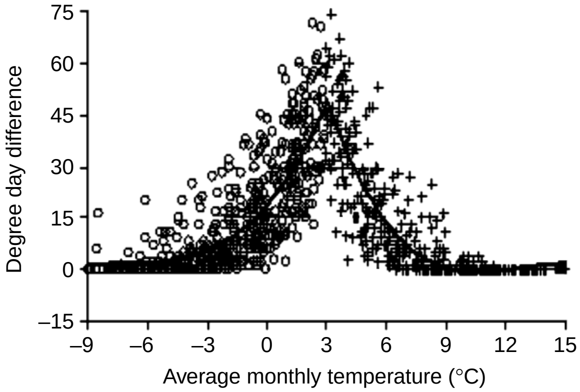

Figure 1 | Distribution of the degree-day difference according to monthly average temperature. Circle symbols are for temperature values less than 3°C and + symbols are for temperature values greater than or equal to than 3°C. Solid lines represent the best non-linear regression fit (Freund *et al.* 2003) to the data values.

CASA uses minimum and maximum monthly temperatures as model inputs, which makes it possible to use the monthly temperature range as a proxy for variance of daily surface temperatures over any given month. Figure 2 shows that, by breaking up the scatter plot in Figure 1 by monthly temperature range, it was possible to estimate the degree-day difference with greater accuracy. Figure 2(a) contains data for the points that have a monthly temperature range between 0 and 10°C. Similarly, the monthly temperature ranges for Figure 2(b,c) are 11–15°C and 16–20°C, respectively. These graphs reveal that the degree-day difference is more pronounced as the average monthly temperature range increases. Between 75% and 87% of the variance in the degree-day difference is explained by taking monthly temperature range into account in conjunction with average monthly temperature. These results and the root mean squared error values are summarized in Table 1.

In short, the average monthly temperature was used to make an initial degree-day calculation. A set of regression formulas were used to compute what degree-day difference needs to be added to the initial degree-day calculation so that it better approximates the true degree-day amount (T). This degree-day total can then be multiplied by the degree-day factor (a) in order to calculate the potential melt depth (S_m). CASA simulates the snow pack depth (as snow water equivalence) for each pixel, so the potential melt depth is then subtracted from this amount and the result is added to the runoff total for that pixel.

Snow–rain partitioning

Auer (1974) reported that the surface air threshold temperature for a 50% to 50% chance of precipitation falling as snow versus rain is 2.2°C. CASA's snow-rain threshold algorithm was modified based on a regression analysis of average monthly temperatures and the

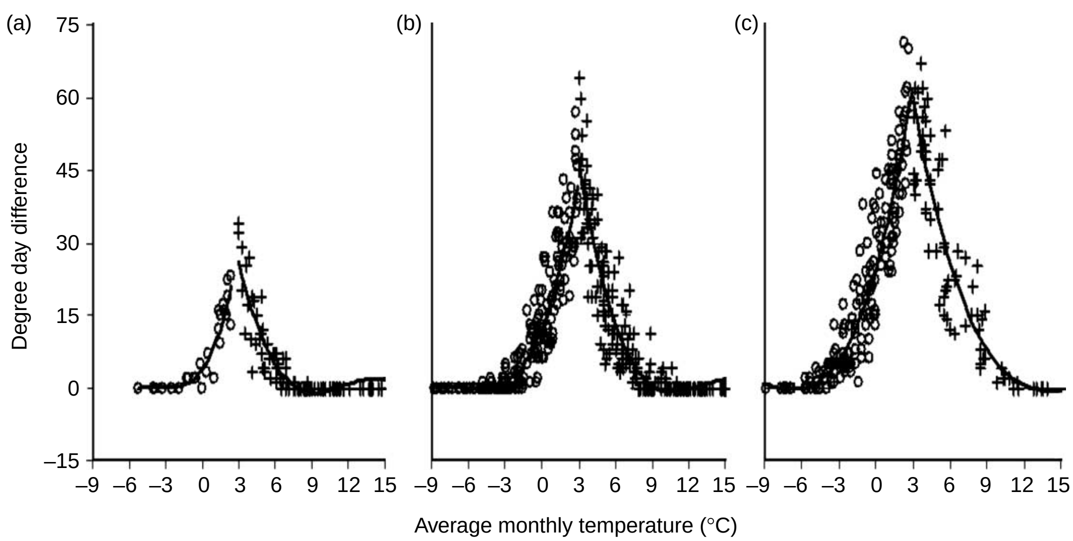

Figure 2 | Regression plots to predict the degree-day difference using two covariates, average monthly temperature at three different monthly temperature ranges (a) 0–10°C, (b) 11–15°C and (c) 16–20°C. Circle symbols are for temperature values less than 3°C and + symbols are for temperature values greater than or equal to than 3°C. Solid lines represent the best non-linear regression fit (Freund *et al.* 2003) to the data values, as described in Table 1.

Table 1 | Regression equations for the degree-day difference using two covariates, average monthly temperature at four different monthly temperature ranges (a) 0–10°C, (b) 11–15°C, (c) 16–20°C and (d) 21 + °C

		Less than 3°C			Greater than 3°C		
		Degree-day difference	DF Adj. R^{2*}	RMSE†	Degree-day difference	DF Adj. R^{2*}	RMSE†
Monthly temp. range (°C)	0–10	$-1.09 + 5.3e^{(x/1.68)}$	0.847	2.94	$-0.52 + 201.48e^{(x/-1.59)}$	0.8481	2.92
	11–15	$-3.02 + 15.18e^{(x/2.65)}$	0.8275	5.62	$-0.8 + 222.38e^{(x/-2.09)}$	0.8702	5.12
	16–20	$-5.65 + 29.53e^{(x/3.4)}$	0.8694	6.59	$-4.83 + 142.21e^{(x/-3.89)}$	0.8351	8.92
	21 +	$-7.5 + 41.33e^{(x/5.39)}$	0.7518	7.33	N/A		

*Degrees of freedom adjusted R^2.
†RMSE: root mean square error.

percentage of days within each month that are below the snow–rain threshold. The temperature data used here were described in the previous section of the paper, except that these records were restricted to the months of November through February. Previously, the CASA model would designate all the precipitation in a month as either all snow or all rain, depending on the average monthly temperature. Using a linear regression formula derived from the scatter plot in Figure 3, the model now partitions the monthly precipitation into a percentage of snow and rain. This new approach mimics how precipitation that occurs near or slightly above freezing naturally falls as a combination of snow and rain.

An assumption that is inherent in using the percentage of days below and above the snow–rain threshold to partition precipitation into rain and snow is that precipitation has an equal chance of falling on any day of the month. However, there can be patterns that violate this assumption. For instance, our analysis of DAYMET precipitation data in the Sierra Nevada showed that only 10%

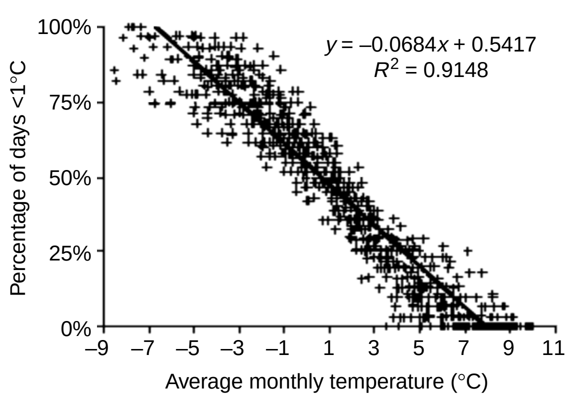

Figure 3 | Regression plot based on average monthly temperature for the proportion of days in a month (November–February, 19802003) for which daily average temperature was less than 1°C.

of precipitation events in November occur within the first week of the month. Another pattern encountered was that daily average temperatures are roughly 0.5°C (in December) to 2.5°C (in November) cooler on days that have precipitation events. These observations justify the refinement of snow–rain thresholds anywhere hydrologic flow estimations are undertaken in applications of the CASA model.

MODEL EVALUATION: STATEWIDE RESULTS FOR 1982–1990

Gauge station data sources and geographic distribution

For comparisons to CASA-HYDRA predictions, California gauge station data for river flow rates was downloaded from the USGS (2008). These data represent actual gauge flow values that were not adjusted to simulate natural flows. Excluding any gauge record that did not have at least 10 years of data, a total of 520 station records were found to have no missing data during our study period (1982–1990). The locations of each gauge in this set of 520 were compared to the predicted river courses in HYDRA. The total number of gauge records was cut down to 354 after elimination all of the gauges that fall directly on a dam feature. Another 18 gauges records were eliminated because their watershed extended beyond California's state border or a large portion of the basin was in an urban area, yielding a subset of 336 gauge station records that were used for CASA-HYDRA validation analysis (Figure 4).

For inter-annual analysis, a subset of 233 gauges was considered where the HYDRA watersheds could be correctly delineated at 1-km resolution. In the majority of

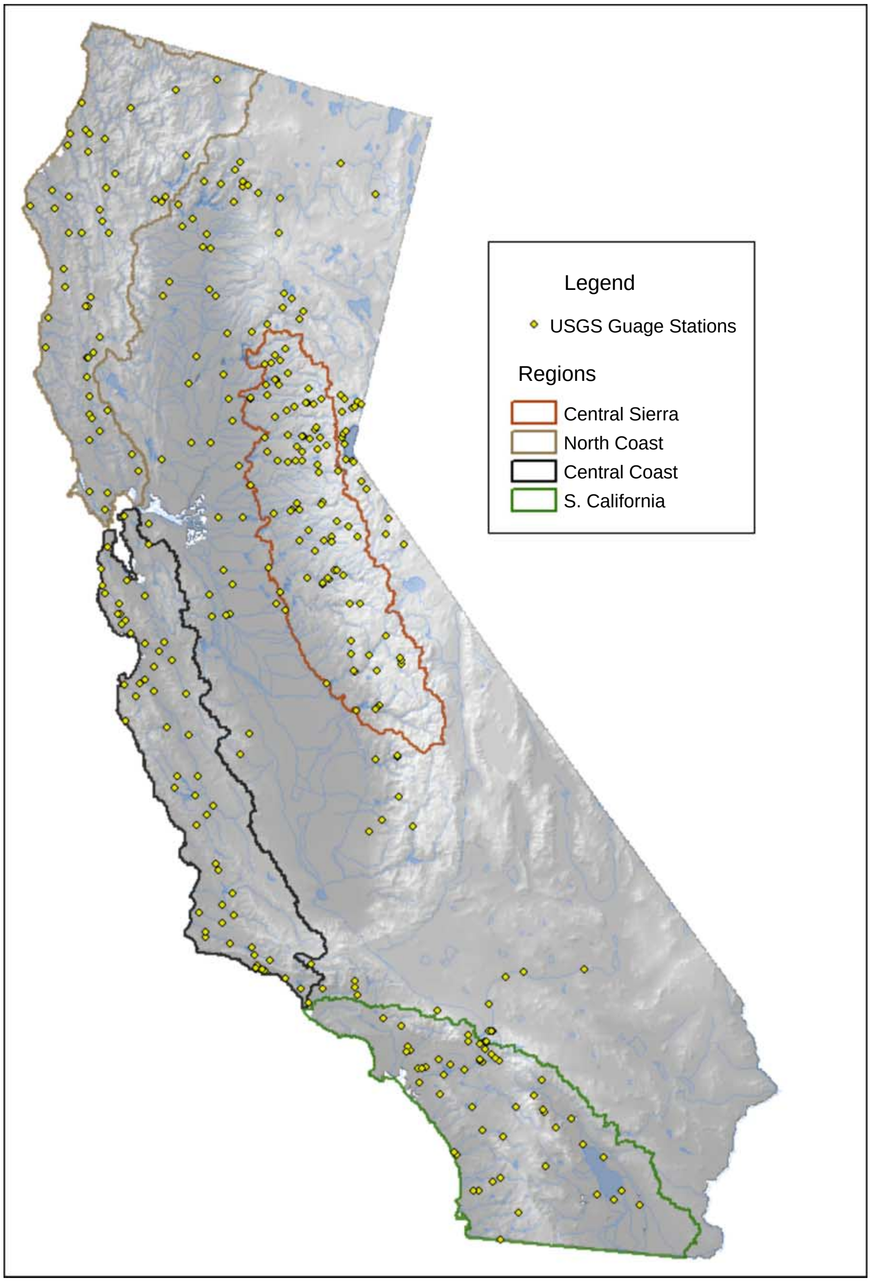

Figure 4 | Distribution of 336 USGS gauge station locations used for evaluation of the CASA-HYDRA river flow model.

the cases where the watershed could not be correctly delineated from a 1-km grid, the location of the gauge station and the HYDRA river course were off by more than one pixel. However, there were also some situations where the gauge and the river corresponded, but there was an error (in at least 10% of the basin's total area) higher in elevation within the watershed. Out of the subset of 233 gauges, analysis was focused further on a total of 42 gauges that did not have any significant upstream diversions or dams on their river courses.

This organization and quality assessment of California river gauge data for model comparisons is in itself an original and unique contribution of our present study. The historical comparisons that follow include analysis of the timing and magnitude of river flow rates across the state system of station gauges in a manner that can reveal land use impacts, potential patterns of flooding, and extreme climate events in large river basins over years to come.

To generate comparable model outputs over the period 1982–1990, the HYDRA model was next initialized with inputs of map layers that define the extent and depth of lakes in the study area (State of California 1999). The model's initialization process involved setting the volume of these lakes to their maximum estimated capacity. The remainder of the study area was initialized by running the model for three years with CASA soil drainage data from 1982, which was a relatively wet year in California.

The Pearson product-moment correlation coefficient (R^2) was used as a test of significant association between the model and gauge flow time series. Following the gauge analysis methods described by Potter *et al.* (2004), the statistical significance of correlations is dependent on the number of observations considered independent in a time series dataset. In all cases, the significance levels of a correlation were determined on the basis of degrees of freedom equal to $n - 2$ years for each discharge station record. For example, with a sample size of $n = 9$ years, which conservatively minimizes all temporal autocorrelation effects in monthly discharge and climate time series data, any value of $R^2 > 0.44$ or $R^2 > 0.64$ can be considered significant at the $p < 0.05$ and $p < 0.01$ confidence levels, respectively (i.e. two-tailed test of significance).

Model comparisons to statewide gauge station data

Based on CASA-HYDRA model predictions of monthly flow rates across 336 stream gauges statewide, the overall (multi-year) model-to-measurement correlation between monthly flows was $R^2 = 0.72$ (Table 2). The CASA-HYDRA model output was 15% higher across all 336 stream gauges than the measured monthly flow records over the period 1982–1990. It is plausible that the model would predict higher flow rates statewide than was measured at the gauge locations, due mainly to regular water diversions for crop and pasture irrigation purposes in the valley growing regions of the state. The CASA-HYDRA model does not yet account for irrigation demands on surface water flows but can readily do so in future model runs

Table 2 | Correlation R^2 values for monthly model flow comparison to 336 gauge station records at locations across the state. The four regional comparisons do not add to the statewide gauge number because gauges in other regions of the state were included in the statewide results

	No. gauges	Yearly	Winter	Spring	Summer	Fall
Statewide	336	0.72	0.69	0.70	0.73	0.80
North coast	48	0.94	0.99	0.93	0.91	0.97
Central coast	56	0.74	0.86	0.72	0.42	0.42
South California	51	0.59	0.39	0.84	0.43	0.22
Sierra	91	0.73	0.69	0.75	0.71	0.61

based on cropped land cover maps already used in the CASA model.

On a seasonal basis, the statewide CASA-HYDRA model predictions showed the lowest error during the summer and fall periods and the highest error during the winter and spring periods (Figure 5). To break down these results further by regions of the state (Figure 4), the model predictions for gauges located on the state's North Coast and Sierra regions showed errors distributed fairly evenly throughout the seasons, whereas the model results for Central Coast and Southern regions showed higher errors mainly during the summer and fall seasons (Table 2).

Month-to-month time-series plots for the entire state and further broken out for the four separate regions revealed that model-gauge flow disparity during the winter and spring periods of the years 1984, 1987, and 1988 (Figure 6(a)) were the most conspicuous contributors to the overall regression results in Table 2. Gauge flow records confirm that 1987 and 1988 were the driest years statewide in the time series used in this study (Figure 6(b)).

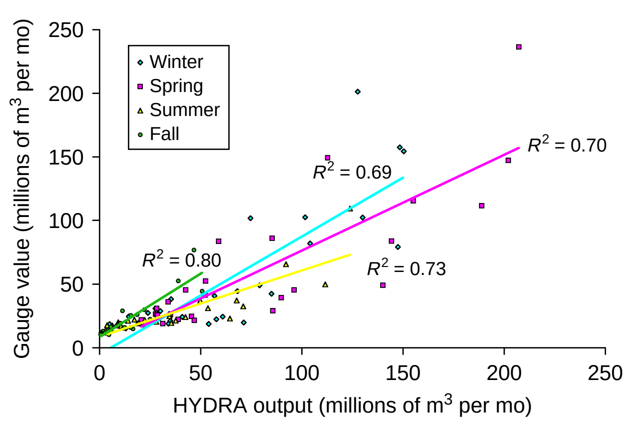

Figure 5 | Seasonal breakdown of the statewide CASA-HYDRA model predictions plotted against gauge flow records from 1982 to 1990.

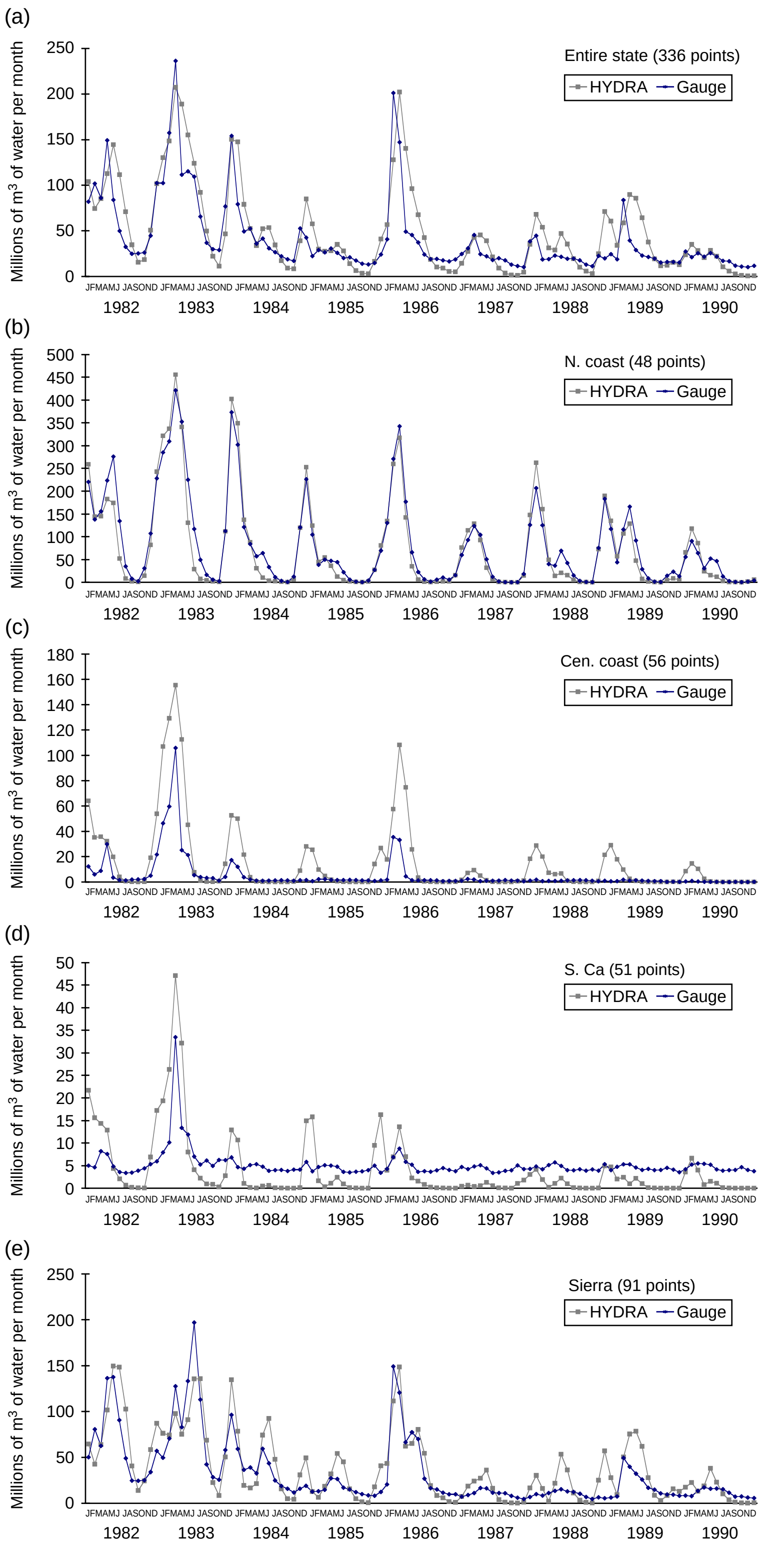

Figure 6 | Monthly time-series plots of CASA-HYDRA model predictions and monthly gauge flow records for the entire state and further broken out for the four separate regions.

The notable disparity in timing of the CASA-HYDRA model predictions lagging one month behind the measured gauge flow records during the winter and spring periods was most easily detected in the time-series plots for Central Coast and Southern regions (Figure 6(c,d)). Furthermore, it was apparent that the CASA-HYDRA predictions could not compensate for large local irrigation water diversions in the Central Coast region, nor for managed water additions from surrounding regions into the Southern region of the state.

As a confirmation of the potential influence of irrigation water management and major storage impoundments on region-wide gauge flow records, statewide comparisons were narrowed to include just the 42 gauges that did not have any significant upstream diversions nor dams on their river courses. As expected, the overall (multi-year) model-to-measurement correlation between monthly flows increased substantially from $R^2 = 0.72$ to $R^2 = 0.81$, and the observation of peak model predictions lagging one month behind the measured gauge flow records during the winter and spring periods was largely eliminated (Table 3). In this narrowed comparison, the effect of irrigation water diversions was no longer evident in gauge records for the Central Coast region, and summer-fall water additions from surrounding regions into the Southern region no longer resulted in model-gauge flow disparities. Moreover, peak model predictions lagging one month behind the measured gauge flow records during the spring months in the Sierra region were corrected as well, presumably by eliminating rivers from the comparison on which large power-generating impoundments are designed to retain snow melt runoff and release reservoir water down streams gradually over the summer months.

Table 3 | Correlation R^2 values for narrowed monthly model flow comparison to include the only gauges that did not have any significant upstream diversions nor dams on their river courses. The four regional comparisons do not add to the statewide gauge number because gauges in other regions of the state were included in the statewide results

	No. gauges	Yearly	Winter	Spring	Summer	Fall
Statewide	42	0.81	0.69	0.76	0.86	0.91
North coast	17	0.79	0.67	0.73	0.79	0.92
Central coast	4	0.83	0.87	0.81	0.76	0.74
South California	4	0.66	0.44	0.94	0.42	0.37
Sierra	5	0.72	0.60	0.76	0.74	0.69

The close match of CASA-HYDRA model predictions to monthly gauge flow records in the North Coast and Sierra regions (Figure 6(b,e), respectively) suggests that the best results from the model in terms of both magnitude and seasonal timing of flows were expected in regions where annual precipitation amounts were highest, and (perhaps coincidently) forested land cover was most homogeneous. This finding is reinforced by model results for the high flow years of 1983 and 1986 (Figure 6(a)), during which winter and spring CASA-HYDRA model to gauge flow errors averaged less than 10%, compared to typical error levels of 15–20% during the same month of surrounding years.

BASIN-SCALE RESULTS AND ANALYSIS OF LAND COVER EFFECTS

Analysis of land cover impacts and related water management effects on prediction of historical river flows was focused in greater detail on four selected basins that span the state from the North Coast to the Central Coast and across to the Sierra region. The four river basins selected for this more detailed analysis, the Eel, American, Tuolomne, and Santa Ynez (Figure 7), vary widely in climate and land cover, as well as water management practices. CASA-HYDRA predictions of monthly river flow rates were compared here to all individual gauge records in each of these basins to assess model performance starting from closest to the headwaters of each river to the farthest gauged location downstream close to where the channel either empties in to ocean (Eel and Santa Ynez) or joins the larger river system in the Central Valley (American and Tuolomne).

North coast Eel River basin

The Eel River flows northwest though California's North Coast and empties into the Pacific Ocean just south of Humbolt Bay (Figure 8(a)). Originating in the center of the Mendocino National Forest, the main stem of the river flows for 322 km through a watershed that totals 9,450 km^2 (Mount 1995). The highest elevations in the basin are just

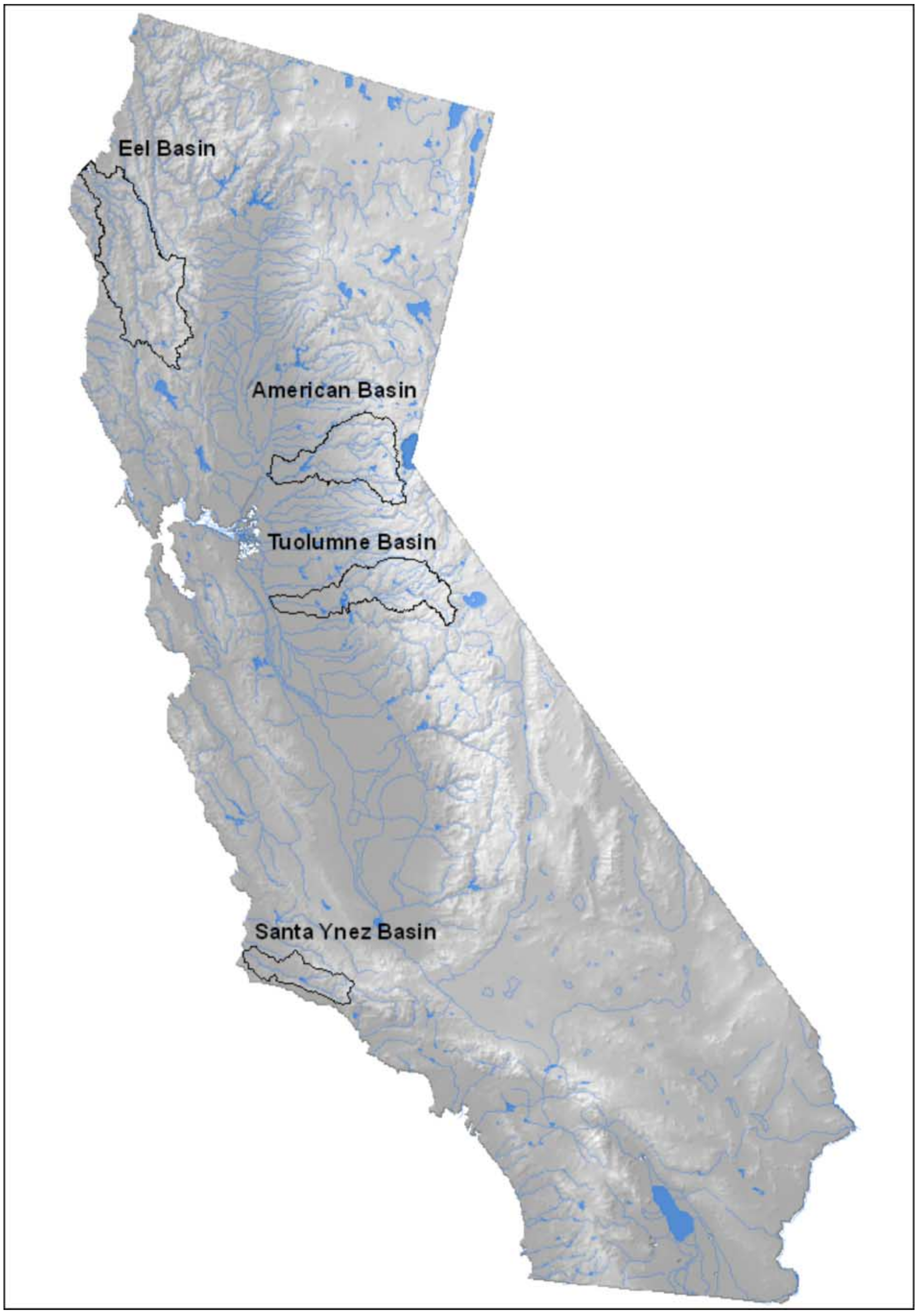

Figure 7 | Four river basins selected for detailed analysis of CASA-HYDRA flow predictions.

over 2,300 m and are located in the South Yolla Bolly Mountains on the eastern border of the watershed. Portions of the Eel River are designated as a Wild and Scenic River (Carle 2004). The Eel basin is in the wettest region of the state. Based on PRISM data for 1960–1990, the average yearly precipitation in the Eel River basin is 133 cm, ranging from 85 cm in the southeast corner to as much as 169 cm further north.

Over 65% of the basin is categorized as forest and a great majority of this area is evergreen coniferous forest (NLCD 1992), including the Coastal Redwood for which the region is famous (Figure 8(a)). Herbaceous grasses, which

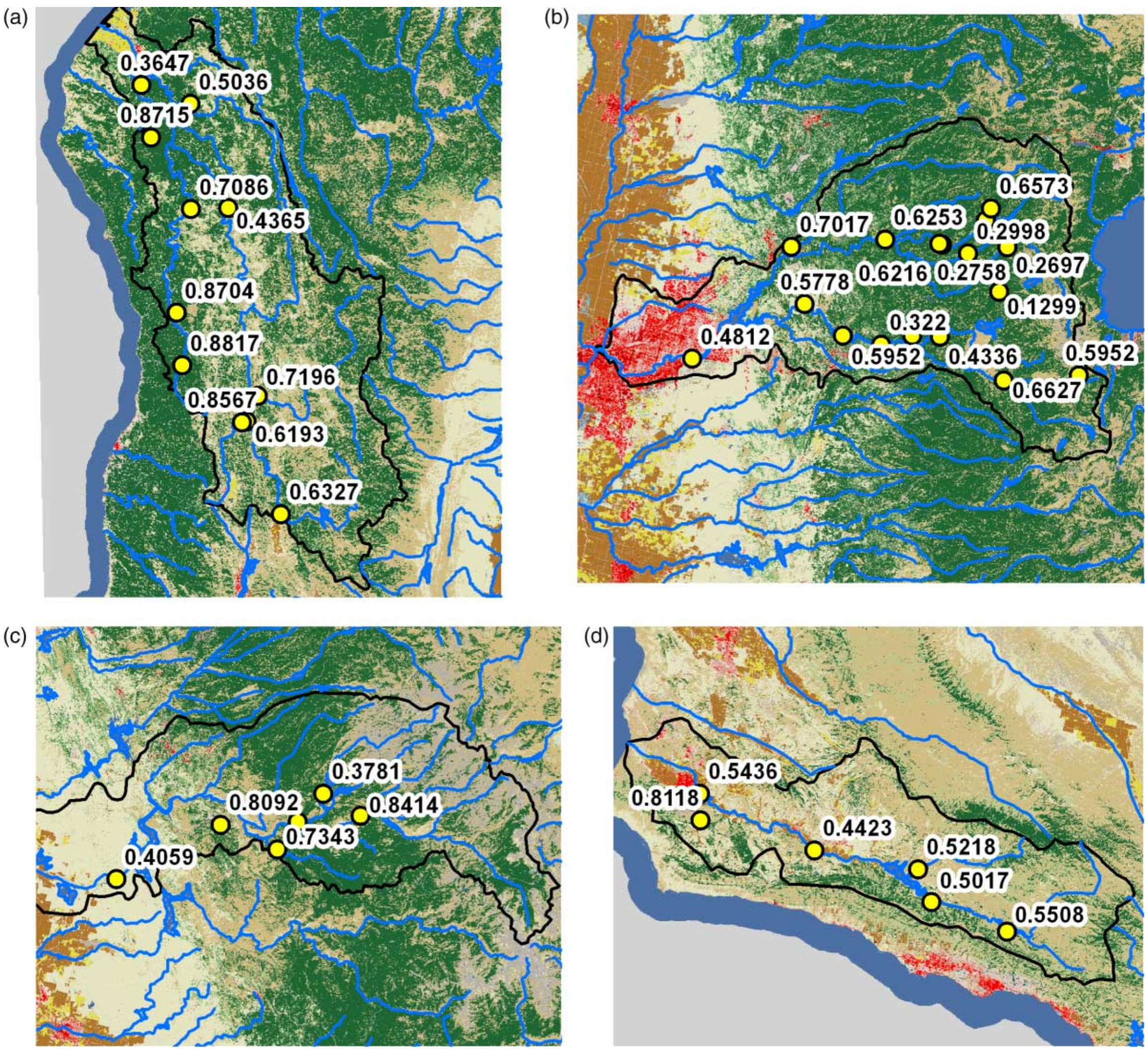

Figure 8 | Land cover, surface water routing, and correlation values between monthly gauge station flows and CASA-HYDRA predictions in four river basins shown in Figure 7. Basin maps are (a) Eel River, (b) American River, (c) Tuolumne, and (d) Santa Ynez. Cover classes from the USGS National Land Cover Database (NLCD 2001) are forest (green), shrubland (tan), grassland (yellow), bare ground (white), cropland (brown), urban (red), and water (blue).

comprise 19% of the basin, typically appear on unstable soils and rock types that are prone to erosion, particularly mass movements (NLCD 1992; Mount 1995). The only significant diversion that occurs within the Eel River watershed is at Lake Pillsbury, about 100 km downstream from its headwaters. Of the approximately 5.6 m^3/s flow that is diverted, the majority is pumped south into the Russian River, but some of the water is used for immediate irrigation needs (USGS 2007).

At 8 out of 11 available stream gauge stations in the Eel River basin, CASA-HYDRA predictions of monthly flow rates over the period 1982–1990 were closely correlated, at $R^2 > 0.55$ (Figure 8(a)). CASA-HYDRA predictions of monthly flow rates were all highly correlated $R^2 > 0.7$) with gauge flows through the western-central portion of the Eel River basin. At two lower-basin gauge locations (Scotia–USGS 11477000 and Fort Seward–USGS 11475000) where the initial results were not as strong, the correlation value increased to nearly $R^2 = 0.8$ when the CASA-HYDRA flow predictions are advanced by just one month. This result suggests that the CASA model controls over precipitation pathways through steep heavily forested watershed sub-basins require minor refinements to permit faster transmission downstream.

Northern Sierra American River basin

From its headwaters at the crest of the Sierra Nevada, the American River flows in a westerly direction for approximately 426 km until it converges with the Sacramento River in California's state capital (Mount 1995), as shown in Figure 8(b). The basin encompasses 5,591 km^2 and an elevation range from 3,170 m to nearly sea level (NAS 1995). In addition to being a crucial water source for numerous municipalities and irrigation districts, the American River is also the most heavily used recreational river in California (LARTF 2002).

Precipitation events generally come from the west, and there is a large orographic effect as storms move up the elevation gradient of the Sierra Nevada. For example, average precipitation in Sacramento is 46 cm while nearly 178 cm falls at the crest of the American River basin (NAS 1995). Consistent with a wet winter, flow timing is dominated by rainfall in the lower elevations in the winter and early spring. In late spring and summer, by contrast, snow melt from the upper elevations contributes to the majority of the river's runoff (Dettinger *et al.* 2004). The American River straddles the snowfall-dominated watersheds in the high Sierra further south and the rainfall-dominated watersheds in the lower elevations to the north. As a result, the American River is particularly prone to flooding (Dettinger 2005).

Coniferous forests, which are concentrated in the upper elevations of the Sierra, comprise 54% of the basin. Herbaceous grasses (6%), hardwood forests (15%), and shrub lands (8%) dominate the Sierra foothills (Figure 8(b)). The lowest reach of the American River meanders through Sacramento, CA, accounting for the largest contribution to the 10% of urban land use in the basin (Roy *et al.* 2006). Within this reach, which was formerly marshland, the river is almost exclusively confined by levees (NAS 1995). Agriculture, which is concentrated in the Central Valley, comprises less than 1% of the American River watershed (Roy *et al.* 2006).

The American River contains numerous dams and pipeline diversions, mainly for electric power generation. Moreover, urban growth continues in Sacramento and in many small towns that dot the upper reaches of the basin. The North Fork of the American River has been largely spared these urbanization impacts because of it relative inaccessibility and because it was designated a Wild and Scenic River in 1978 (NAS 1995).

At 9 out of 17 available stream gauge stations in the America River basin, CASA-HYDRA predictions of monthly flow rates over the period 1982–1990 were closely correlated, at $R^2 > 0.55$ (Figure 8(b)). At gauge locations where the initial correlation results were not as strong, including South Fork (USGS 11443500) and Silver Creek (USGS 11441900) near Camino Diversion Dam, CASA-HYDRA overestimated river flow rates consistently, only to closely predict flow rates again ($R^2 > 0.57$) just downstream of the locations where water re-enters the river channel by pipeline from the Diversion Dam (USGS 2007). The pattern also was evident on the Middle Fork of the basin, where CASA-HYDRA predictions improved markedly downstream of the Foresthill gauge (USGS 11427770), below the re-entry location for the pipeline diversion that carries water from Sugar Pine Reservoir over the Foresthill Divide area. In contrast, model correlations on the undiverted North Fork of the basin were the highest anywhere in the watershed at $R^2 = 0.7$ (USGS 11427000). These results suggests that the CASA-HYDRA model accurately predicts monthly and inter-annual surface water flows in the American River basin when the analysis accounts for pipeline diversions that greatly diminish natural flow rates at nearly half the gauge locations on the South and Middle Forks.

Southern Sierra Tuolomne River basin

The Tuolumne River flows from the crest of the Sierra Nevada within Yosemite National Park westward to its confluence with the San Joaquin River in the southern half of California's Central Valley (Figure 8(c)). The Tuolumne is approximately 210 km in length and it drains a 5,075 km^2 watershed (SFCCPD 2007). As the largest tributary on the San Joaquin River, the Tuolumne River is an important component of the state's water budget. Approximately 85% of San Francisco's water supply, for instance, comes from the Hetch Hetchy Reservoir System, which is a series of reservoirs in the upper reaches of the Tuolumne River (Toch 2000).

The mountainous terrain of its headwaters is characterized by steep valleys with granite river channels.

The gradient of the Tuolumne and its tributaries in these reaches typically ranges between 2 and 6%. Since the watershed of the Tuolumne River upstream of the Sierra foothills is protected by National Forest and National Park land, the land use in this area has not been significantly altered by human impact (SFCCPD 2007; Figure 8(c)). In contrast to its headwaters, the lower Tuolumne River has been greatly impacted by irrigated agriculture, grazing, and gravel mining. For example, the area categorized as riparian vegetation along the lower reach of the river has declined by over 83% since Euro-American habitation (SFCCPD 2007).

Annual runoff in the Tuolumne River basin is highly variable, as is typical in the western USA (Carle 2004). Between 1918 and 1991, for instance, the average annual unimpaired runoff at Don Pedro Reservoir in the Sierra foothills has ranged between 0.48 billion m^3 and 4.74 billion m^3 (SFCCPD 2007). Reservoirs and diversions have significantly altered the magnitude and seasonal flow of the Tuolumne River. Today, 32.5% of the natural flow of the Tuolumne is diverted at Hetch Hetchy and about 67% of the lower Tuolumne River water is diverted. Moreover, the seasonal pattern has shifted so that spring flows are delayed into the dry summer months. Consequently, peak flows have been greatly diminished. The 20-year return-period flood flow on the Tuolumne River downstream of Don Pedro Reservoir has declined from 1,671 m^3/s to 341 m^3/s (SFCCPD 2007).

At four out of six available stream gauge stations in the Tuolomne River basin, CASA-HYDRA predictions of monthly flow rates over 1982–1990 were highly correlated, at $R^2 > 0.68$ (Figure 8(c)). At gauge locations where the initial correlation results were not as strong, namely at La Grange Dam below Don Pedro Reservoir (USGS 11289650) and below Hetch Hetchy (USGS 11277300), CASA-HYDRA overestimated river flow rates consistently, only to closely predict flow rates again ($R^2 > 0.69$) at Cherry Creek near Mather (USGS 11278400) well downstream of the Hetch Hetchy diversion (USGS 2007). At the gauge location highest in the basin (USGS 11276500), the model tracked measured flow rates with just 1% error over the nine-year period of 1982–1990. Nevertheless, CASA-HYDRA predictions had a tendency to underestimate peak spring runoff rates in these high Sierra watersheds that are covered by a mixture of forest and alpine meadows, which again implied model controls over snow melt through steep sub-basins require minor refinements to permit faster runoff flow downstream.

Central Coast Santa Ynez River basin

The Santa Ynez River is located on the southern edge of California's Central Coast (Figure 8(d)). Its headwaters are between the San Rafael Mountains to the east and north and the Santa Ynez Mountains to the south. The river travels approximately 113 km in its westward descent through Lompoc Valley before it reaches the Pacific Ocean (Mount 1995). Within this 2,342 m^2 watershed, the total elevation gain is an impressive 2,010 m.

As a Mediterranean climate, the Santa Ynez basin experiences wet winters and dry summers. An average of approximately 65 cm of precipitation falls each year in the southern extent of the Central Coast (Mount 1995). Although the coastal mountains are not nearly as high as the Sierra, their steep terrain results in a significant orographic effect. Some snow falls on the highest peaks in the winter, but this accumulation represents an insignificant contribution to the annual discharge of the basin (Mount 1995).

Covering 35% of the basin, chaparral is the most prevalent vegetation type and it grows throughout the entire watershed (Figure 8(d)). Evergreen and mixed forests, which total 25% of the basin's area, are concentrated in the mountainous headwaters in the east of the basin. The lower elevations in the western half of the watershed are dominated by herbaceous grasses, which comprise 29% of the basin. Seven percent of the watershed is in cultivated cropland (NLCD 1992).

Just outside of Lompoc, CA, roughly 14 km upstream of the river's mouth, the annual mean discharge (for water years 1953–2007) was 2.2 m^3/s. Indicative of heavy municipal and irrigation demands, the annual mean discharge (for water years 1952–2007) was 3.7 m^3/s for a gauge that is about 8 km upstream of Lompoc, CA (USGS 2007). Typical of many southern California rivers, peak flows occur in the winter months and the Santa Ynez will frequently run dry in the late summer (USGS 2007). Central Coast rivers, such as the Santa Ynez, are prone to flooding during intense winter storms because they are usually small and steep, resulting in very short lag times and high peak runoffs (Mount 1995).

At only two out of six available stream gauge stations in the Santa Ynez River basin, CASA-HYDRA predictions of monthly flow rates over 1982–1990 were closely correlated, at $R^2 > 0.55$ (Figure 8(d)). At the other gauge locations where the correlation results were not as strong ($R^2 > 0.44$), CASA-HYDRA overestimated river flow rates consistently, with the exception of predicted flows during the exceptionally wet months of 1983 that closely followed peak winter rates at all gauges in the basin. It appears therefore that in basins such as this with high municipal and irrigation demands on river flows, CASA-HYDRA must be refined to more accurately account for these diversions to urban and agricultural land cover areas during all but the wettest rainfall seasons.

DISCUSSION AND FUTURE MODEL APPLICATIONS

Results from CASA-HYDRA simulations support the hypothesis that modeled flow rates are consistently more accurate (compared to historical river flow records) in watersheds where satellite mapping specifies a more homogeneous land cover composition (mainly forest or shrubland) than in watersheds with highly mixed agricultural and urbanized land cover types. Results also support the hypothesis that modeled flow rates are significantly less accurate (compared to historical flow records) in watersheds where river diversions for generation of hydroelectric power are prevalent, compared to rivers with no diversions for generation of hydroelectric power. These hypothesis tests together imply that future hydrologic modeling in California must rigorously account for diversions of the State's river courses to meet the changing needs for cropland irrigation, flood control, and electric power generation.

There have been numerous previous studies published on regional-scale modeling of surface hydrologic flows in California. In contrast to our application of the CASA-HYDRA model to historical conditions, the majority of these previous simulation studies have focused on projections of isolated impacts of future climate change on water availability in the state. For instance, Knowles & Cayan (2002) used temperature anomalies from climate model projections to drive a combined model of watershed hydrology and estuarine dynamics for the San Francisco Bay. Results implied loss of about half of the average April snow pack storage by 2090, with associated increases in winter flood peaks.

Maurer & Duffy (2005) applied the variable infiltration capacity (VIC) model in California, which is a distributed, physically based hydrologic model that balances both surface energy and water over a grid, typically run at a resolution between a fraction of a degree and several degrees latitude by longitude. A distinguishing characteristic of VIC is its use of a "mosaic" scheme, which allows a statistical representation of spatial variability in topography and vegetation/land cover at a sub-grid scale. This is important when simulating accumulation and ablation of snow in more complex terrain. The VIC model also features a nonlinear simulation of slow runoff response (baseflow), and explicitly treats vegetation's effects on the surface energy balance (Maurer & Duffy 2005). The VIC simulations have implied that, while the different climate change scenarios predict significantly different regional climate responses to increasing atmospheric CO_2, hydrological responses were robust across future climate projections: decreases in summer low flows and increases in winter flows, and a shift of flow to earlier in the year. Summer flow decreases became consistent across models at lower levels of greenhouse gases than increases in winter flows.

Vicuna *et al.* (2007) also used the VIC model to derive inflows to major reservoirs in the California Central Valley. Historical inflows were used as inputs to the water resources model CalSim II and modified to represent the climate change perturbed conditions for water supply deliveries, reliability, reservoir storage, and changes to variables of environmental concern. Results showed greater negative impacts to California hydrology and water resources than previous assessments of climate change impacts in the region. These impacts translate into smaller stream flows, lower reservoir storage, and decreased reliability of water deliveries.

Finally, CALVIN (California Value Integrated Network), an integrated economic-engineering optimization model of California's inter-tied water system, was developed for water policy, planning, and operations studies (Draper *et al.* 2003; Tanaka *et al.* 2006). The generalized network flow-based optimization model minimizes the economic operating and scarcity costs of water supply, subject to water-balance, capacity, and environmental constraints for a range of hydrologic and operational conditions represented by a monthly 72-year time series of inflows. The CALVIN model is an enhancement of the HEC-PRM (Hydrological Engineering Center Prescriptive Reservoir Model) code developed by the US Army Corps of Engineers in 2005. In 12 climate change scenarios examined with CALVIN, increases in winter season (November–March) flows were projected to spill over existing storage facilities. In all cases, spring snowmelt was greatly decreased with climate warming, and winter flows were generally increased.

To complement these previous modeling studies of future climate-driven change in major river basins of the state, this paper outlines the potential for applying the CASA-HYDRA model to examine the influences of past and future land cover changes in California, many of which can interact strongly with climate change trends. Firstly, the CASA model has been used in previous studies of irrigation and fertilizer practices in California's major valley crop growing regions (Potter *et al.* 2001, 2003). In this approach, each of the 10–12 major crop types inventoried regularly by the Department of Water Resources (DWR 1998) were uniquely represented in the CASA modeling application for water use demands. The losses of surface water to evapotranspiration in all cropped areas of the state must be next added to the CASA-HYDRA model at the highest possible resolution of land use mapping offered by the DWR. New runs of our model will be used to estimate the changes in irrigation water demand with projected changes in climate (both predicted surface temperature and precipitation rates) over the next 100 years.

Our CASA-HYDRA model is now being adapted as well to simulate the hydrologic effects of mature (undisturbed for > 50 years) forest versus burned forest cover in selected drainage basins in the western US region. According to Westerling *et al.* (2006), the frequency of large wildfires has increased in the western United States over the past 25 years, which is strongly associated with increased spring and summer temperatures and an earlier spring snowmelt. Global climate model projections were used by Westerling & Bryant (2008) to predict future fire activity in California, with increasing temperatures promoting greater large fire frequency in wetter, forested areas, based mainly on fuel flammability effects. In this analysis, the largest changes in property damage under the climate change scenarios occurred in wildland/urban interfaces proximate to major metropolitan areas in coastal southern California, the San Francisco Bay Area, and in the Sierra foothills northeast of Sacramento.

Previous research on changes in surface hydrology with wildfire alterations of land cover generally indicate that runoff from a burned catchment is greater than measured flow rates before a fire (Baker 1990; Moody & Martin 2001; Helvey 2007). Sediment yield is often elevated following a forest fire as well, and then begins to decrease as stream channels become stabilized and vegetation recovery on upper slopes improves infiltration capacity. Wildfire directly affects the evapotranspiration/interception regime of a disturbed area by reducing or eliminating vegetation surfaces from which these processes occur (Beschta 1990). The result is decreased losses of precipitation to evapotranspiration, and proportionately more water available to flow through a watershed. Wildfire can modify the infiltration and percolation (movement of water through soil) characteristics of a watershed by removing the organic litter layer (duff) and creating water-repellent layers. Finally, wildfires that reduce the vegetation cover may result in deeper snow packs that melt faster than normal (Skidmore *et al.* 1994). Because the CASA-HYDRA model is build upon the foundation of a detailed and dynamic land cover data set from continuous satellite imaging, it is being applied to evaluate the impacts of changes in evapotranspiration, infiltration, percolation, and snow pack depth in large burned areas of California.

By successfully comparing the CASA-HYDRA model flow results to multiple years of actual river gauge records, this study has established the validity of our large-scale approach to surface hydrologic modeling in the climatically complex and highly managed water resource environment of California. Despite widespread water diversions of the State's river courses for cropland irrigation and electric power generation, careful interpretation of model-gauge flow comparisons can build the capacity to predict monthly and annual river discharge rates with high confidence.

ACKNOWLEDGEMENTS

The authors thank Michael Coe for HYDRA/THMB model code and assistance in algorithm implementation. We thank Bob Rice for providing degree-day factor data for the Sierra Nevada. This research was supported by a grant to C. Potter from NASA Ames Research Center.

REFERENCES

Auer, A. H. 1974 The rain versus snow threshold temperatures. *Weatherwise 27*, 67.

Baker, M. B., Jr. 1990 *Hydrological and Water Quality Effects of Fire*. USDA Forest Service. Rocky Mountain Forest and Range Experiment Station. General Technical Report GTR-RM-191, Fort Collins, Colorado, pp. 31–42.

Beschta, R. L. 1990 Effects of fire on water quantity and quality. In *Natural and Prescribed Fire in Pacific Northwest Forests* (ed. J. D. Walstad, S. R. Radosevich & D. V. Sandberg), pp. 219–232. Oregon State University Press, Corvallis, Oregon, USA.

Callaway, R. M. & Davis, F. W. 1993 Vegetation dynamics, fire, and the physical environment in coastal central California. *Ecology* **74** (5), 1576–1578.

Cao, W., Bowden, W. B., Davie, T. & Fenemor, A. 2008 Modelling impacts of land cover change on critical water resources in the Motueka River catchment, New Zealand. *Water Resour. Manage.* **23** (1), 37–151.

Carle, D. 2004 *California Natural History Guide: Introduction to Water in California*. University of California Press, Berkeley and Los Angeles, California.

Coe, M. T. 2000 Modeling terrestrial hydrologic systems at the continental scale: testing the accuracy of an atmospheric GCM. *J. Clim.* **13** (4), 686–704.

Department of Water Resources (DWR) 1998 California Department of Water Resources. Standard Land Use Legend. Division of Planning, Sacramento, CA. [Available online at http://www.water.ca.gov/landwateruse/]

Dettinger, M. D. 2005 A long-tern (~50 yr) historical perspective on flood-generating winter storms in the American River basin. In *Proceedings of the California Extreme Precipitation Symposium, April 22, 2005.*

Dettinger, M. D. & Cayan, D. R. 1995 Large-scale atmospheric forcing of recent trends toward early snowmelt runoff in California. *J. Clim.* **8** (3), 606–623.

Dettinger, M. D., Cayan, D. R., Meyer, M. K. & Jeton, A. E. 2004 Simulated hydrologic responses to climate variations and change in the Merced, Carson, and American River Basins, Sierra Nevada, California, 1900–2099. *Clim. Change* **62** (1–3), 283–317.

Draper, A. J., Jenkins, M. W., Kirby, K. W., Lund, J. R. & Howitt, R. E. 2003 Economic-engineering optimization for California water management. *J. Water Resour. Plann. Manage.–ASCE* **129** (3), 155–164.

Freund, R., Littell, R. & Creighton, L. 2003 *Regression Using JMP*. SAS Institute, John Wiley, Hoboken, NJ.

Helvey, J. D. 2007 Effects of a north central Washington wildfire on runoff and sediment production. *J. Am. Water Resour. Assoc.* **16** (4), 627–634.

Inman, D. L. & Jenkins, S. A. 1999 Climate change and the episodicity of sediment flux of small California rivers. *J. Geol.* **107** (3), 251–270.

Knowles, N. & Cayan, D. R. 2002 Potential effects of global warming on the Sacramento/San Joaquin watershed and the San Francisco estuary. *Geophys. Res. Lett.* **29** (18), 1891.

Lower American River Task Force (LARTF) 2002 Lower American River: River Corridor Management Plan, January 2002.

Lundquist, J. D., Dettinger, M. D. & Cayan, D. R. 2005 Snow-fed streamflow timing at different basin scales: case study of the Tuolumne River above Hetch Hetchy, Yosemite, California. *Water Resour. Res.* **41**, W07005.

Martinec, J. 1975 Snowmelt-runoff model for stream flow forecasts. *Nord. Hydrol.* **6** (3), 145–154.

Martinec, J., Rango, A. & Roberts, R. 1998 Snowmelt runoff model (SRM) User's Manual. *Geographica Bernensia*, 35.

Maurer, E. P. & Duffy, P. B. 2005 Uncertainty in projections of streamflow changes due to climate change in California. *Geophys. Res. Lett.* **32** (3), L03704.

Miller, S. N., Kepner, W. G., Mehaffey, M. H., Hernandez, M., Miller, R. C., Goodrich, D. C., Devonald, K. K., Heggem, D. T. & Miller, W. P. 2002 Integrating landscape assessment and hydrologic modeling for land cover change analysis. *J. Am. Water Res. Assoc.* **38** (4), 915–929.

Miller, S. N., Semmens, D. J., Goodrich, D. C., Hernandez, M., Miller, R. C., Kepner, W. G. & Guertin, D. P. 2007 The automated geospatial watershed assessment tool. *Environ. Model. Softw.* **22** (3), 365–377.

Miller, S. N., Guertin, D. P. & Goodrich, D. C. 2007 Hydrologic modeling uncertainty resulting from land cover misclassification. *J. Am. Water Res. Assoc.* **43** (4), 1065–1075.

Moody, J. & Martin, D. 2001 Initial hydrologic and geomorphic responses following a wildfire in the Colorado Front Range. *Earth Surf. Process. Landforms* **26** (10), 1049–1070.

Mount, J. F. 1995 *California Rivers and Streams: The Conflict Between Fluvial Process and Land Use*. University of California Press, Berkeley and Los Angeles, California.

National Academy of Sciences (NAS) 1995 *Flood Risk Management and the American River Basin: An Evaluation*. The National Academy Press, Washington DC.

National Land Classification Dataset (NLCD) 1992 U.S. Geological Survey, EROS Data Center, http://www.mrlc.gov/ (accessed April 27, 2006).

National Land Cover Database (NLCD) 2001 http://www.mrlc.gov/mrlc2k_nlcd.asp (accessed January 2009).

Potter, C. S., Randerson, J. T., Field, C. B., Matson, P. A., Vitousek, P. M., Mooney, H. A. & Klooster, S. A. 1993 Terrestrial ecosystem production: a process model based on global satellite and surface data. *Global Biogeochem. Cycles* **7** (4), 811–841.

Potter, C., Krauter, C. & Klooster, S. 2001 *Statewide inventory estimates of ammonia emissions from fertilizer applications in California*. Project report to California Air Resources Board, Sacramento, CA. Contract# ID98-76.

Potter, C., Klooster, S. & Krauter, C. 2003 Regional modeling of ammonia emissions from native soil sources in California. *Earth Interact.* **7**, 1–28.

Potter, C. S., Zhang, P., Klooster, S., Genovese, V., Shekhar, S. & Kumar, V. 2004 Understanding controls on historical river discharge in the world's largest drainage basins. *Earth Interact.* **8** (2), 1–21.

Potter, C., Klooster, S., Huete, A. & Genovese, V. 2007 Terrestrial carbon sinks for the united states predicted from MODIS satellite data and ecosystem modeling. *Earth Interact.* **11** (13), 1–21.

Rice, R., Bales, R., Painter, T. & Dozier, J. 2007 Snowcover along elevation gradients in the Upper Merced and Tuolumne River basins of the Sierra Nevada of California from MODIS and blended ground data. In *Proceedings of the 75th Annual Western Snow Conference*.

Roos, M. 1991 A trend of decreasing snowmelt runoff in northern California. In *Proceedings of the 59th Western Snow Conference, Juneau, AK*, pp. 29–36.

Roy, S., Heidel, K., Creager, C., Chung, C. F. & Grieb, T. 2006 *Conceptual model for organic carbon in the Central Valley and Sacramento-San Joaquin Delta, Tetra Tech, Inc, April 14, 2006*. US EPA Final Technical Report.

San Francisco City and County Planning Department (SFCCPD) 2007 *Draft Program Environmental Impact Report for the San Francisco Public Utilities Commission's Water System Improvement Program, Vol. 3*. San Francisco Planning Department File No. 2005.0159E.

Skidmore, P., Hansen, K. & Quimby, W. 1994 Snow accumulation and ablation under fire-altered lodgepole pine forest canopies. In *Proceedings of the Western Snow Conference. Sante Fe, N. Mex., April 18–21, 1994.* Colorado State University, Fort Collins, Colo., pp. 43–52.

State of California 1999 Stephen P. Teale Data Center GIS Solutions Group, CALWATER 2.2.1, http://gis.ca.gov/casil/hydrologic/watersheds/calwater/

Tanaka, S. K., Zhu, T., Lund, J. R., Howitt, R. E., Jenkins, M. W., Pulido, M. A., Tauber, M., Ritzema, R. S. & Ferreira, I. C. 2006 Climate warming and water management adaptation for California. *Clim. Change* **76** (3–4), 361–387.

Thornton, P. E., Running, S. W. & White, M. A. 1997 Generating surfaces of daily meteorological variables over large regions of complex terrain. *J. Hydrol.* **190** (3–4), 214–251.

Toch, S. L. 2000 Water to Drink: Sustaining Watersheds and the People Who Need Them, *USDA Forest Service Proceedings*, RMRS-P-14.

United States Geological Survey (USGS) 2007 Annual Water-Data Reports, http://wdr.water.usgs.gov/ [Accessed August 6, 2008].

USGS DEM 2008 USGS: The National Map Seamless Server. http://seamless.usgs.gov/index.php [Accessed May 27, 2008].

USGS Water 2008 USGS Real-Time Water Data for the Nation. http://waterdata.usgs.gov/nwis/uv [Accessed May 27, 2008].

Vicuna, S., Maurer, E. P., Joyce, B., Dracup, J. A. & Purkey, D. 2007 The sensitivity of California water resources to climate change scenarios. *J. Am. Water Resour. Assoc.* **43** (2), 482–498.

Westerling, A. L., Hidalgo, H. G., Cayan, D. R. & Swetnam, T. W. 2006 Warming and earlier spring increases western U.S. forest wildfire activity. *Science* **313**, 940–943.

Westerling, A. L. & Bryant, B. P. 2008 Climate change and wildfire in California. *Clim. Change* **87**, s231–s249.

Witty, J. H., Graham, R. C., Hubbert, K. R., Doolittle, J. A. & Wald, J. A. 2003 Contributions of water supply from the weathered bedrock zone to forest soil quality. *Geoderma* **114** (3–4), 389–400.

First received 24 June 2009; accepted in revised form 3 February 2010